Iranian Journal of Numerical Analysis and Optimization
Vol. 16, No. 1, 2026, pp 283–303
https://doi.org/10.22067/ijnao.2025.95542.1738
https://ijnao.um.ac.ir/

Research Article

Dynamics and applications of quantum iterative methods

S.K. Nayak*, P.K. Parida and B. Mehta

Abstract

In this article, we introduce a new parametric family of the Quantum iterative method (PFQIM), constructed using the quantum derivative (q-derivative) to solve nonlinear equations. The stability and convergence analysis of the proposed family is analyzed through dynamical graphs. The dynamical and convergence planes of methods are examined using complex and real dynamics, respectively. In complex dynamics, we provide a scaling theorem for PFQIM to study affine conjugacy classes of iterative methods. Moreover, the influence of the q-derivative and the method parameter on stability and convergence is discussed in detail through real dynamics and real-world applications.

AMS subject classifications (2020): Primary 65H05; Secondary 26A33.

*Corresponding author

Received 20 September 2025; revised 21 October 2025; accepted 24 November 2025

Sapan Kumar Nayak
Department of Mathematics, Usha Martin University, Ranchi-835103, India. e-mail: sapannayak7@gmail.com

P. K. Parida
Department of Mathematics, Central University of Jharkhand, Ranchi-83522, India. e-mail: pkparida@cuj.ac.in

Babita Mehta
ICFAI University, Jharkhand, Ranchi-835222, India. e-mail: babita10625@gmail.com

How to cite this article
Nayak, S.K., Parida, P.K. and Mehta, B., Dynamics and applications of quantum iterative methods. *Iran. J. Numer. Anal. Optim.*, 2026; 16(1): 283-303. https://doi.org/10.22067/ijnao.2025.95542.1738

Keywords: Nonlinear equation, q-derivative, Basin of attraction, Scaling theorem, Dynamical plane, Convergence plane, $ACOC$.

1 Introduction

In many areas of science, mathematical models are very important. The billiard ball model of a gas, the Bohr model of an atom, the Lorenz model of the atmosphere, the Lotka-Volterra model of how predators and prey interact, the Schrödinger-type model [16], electrodynamics [1], and so on, are all examples of models based on mathematics. One of the most important tools of modern science is the mathematical model. When these models are applied to specific problems, they typically lead to nonlinear or differential equations, or even systems of equations. The difficulty is that finding exact solutions is extremely challenging if not impossible therefore numerical approximations using iterative methods become necessary. Let

$$S(z) = 0, \tag{1}$$

where $S : \mathbb{C} \to \mathbb{C}$ with $\mathbb{C}$ being the complex plane, and the most popular method is Newton's method, which produces a rational function with unknown dynamics. The dynamical properties of rational functions associated with iterative methods provide valuable information regarding their numerical stability and reliability. Many authors [4, 7, 8, 2, 15, 11, 20] have studied the complex dynamics of different types of methods and revealed their dynamical properties. In the last few years, complex dynamics have played an important role in mathematics, and the dynamical plane helps us to study complex variable rational functions. Later, in 2014, Magreñán [12] has provided a new tool, that is, a convergence plane, to easily understand the real dynamics of iterative methods. As a result, the real dynamics is different from complex dynamics, so many authors have explored the study of the real dynamics of several methods. In this literature, we use the quantum derivative (q-derivative) to study the dynamical behavior of a rational function obtained from the parametric family method (Chebyshev–Halley family method [8]) using complex dynamics as below:

$$\begin{cases} z_0 \text{given}, \\ z_{k+1} = z_k - \left(1 + \frac{0.5 L_S(z_k)}{(1-\delta * L_S(z_k))}\right) \frac{S(z_k)}{S'(z_k)}, \end{cases} \tag{2}$$

where $L_S(z_k) = \frac{S(z_k)S''(z_k)}{(S'(z_k))^2}$ and $\delta \in \mathbb{C}$ is the complex parameter. We obtain the super Halley method (SHM, $\delta = 1$), Halley method (HM, $\delta = 0.5$), Chebyshev method (CM, $\delta = 0$), and

Newton method (NM, $\delta = \infty$). Furthermore, using real dynamics for some real-world phenomena, interesting numerical results have been discussed.

The q-calculus is a branch of mathematics in which the derivative of a function can be taken without limit. It is a combination of mathematics and physics and was first developed in 1908 by Jackson [9]. Then the authors, Jing and Fan [10] introduced the q-Taylor's formula with its q-remainder term. Singh, Mishra, and Pathak [23] explored the q-analogue of the iterative schemes and provided some interesting comparison results with classical schemes. Recently, many authors [21, 18, 22] derived some higher-order multi-step q-iterative methods to solve nonlinear equations and determined the convergence of the methods.

Let us recall some basic definitions and results of the q-calculus for $q \in (0, 1)$, which we have used in our study.

In q-calculus, for $q \in (0, 1)$, the q-integer can be defined as below:

$$\begin{cases} [p]_q = 1 + q + q^2 + \cdots + q^p - 1 = \frac{1-q^p}{1-q} & \text{for } p = 1, 2, 3, \ldots, \\ [p]_q = 1 & \text{for } q = 1. \end{cases} \tag{3}$$

The q-factorial and q-binomial are defined as

$$\begin{cases} [p]_q! = [p]_q [p-1]_q \cdots [1]q, \\ [0]_q! = 1, \\ \binom{p}{m}_q = \frac{[p]_q!}{[m]_q! [p-m]_q!}. \end{cases} \tag{4}$$

Definition 1. Suppose that $S : \mathbb{C} \to \mathbb{C}$ is a continuous function. Then the q-derivative is defined as follows:

$$\begin{cases} D_q S(z) = \frac{S(qz) - S(z)}{qz - z}, & q \neq 1, \\ \frac{d}{dz} S(z) = \lim\limits_{h \to 0} \frac{S(z+h) - S(z)}{h}, & q = 1. \end{cases} \tag{5}$$

Definition 2. The product and quotient of the q-derivative of continuous $S(z)$ and $H(z)$ are

$$D_q(S(z)H(z)) = H(z) D_q S(qz) + S(qz) D_q H(z),$$

$$D_q \frac{S(z)}{H(z)} = \frac{H(z) D_q S(z) - S(z) D_q H(z)}{H(qz) H(z)}, \qquad H(z)H(qz) \neq 0.$$

Definition 3. The q-Taylor's series of a function $S(z)$ about the point z^* defined by Jackson

$$S(z) = \sum_{n=1}^{\infty} \frac{D_q^{(n)}(z-z^*)^n}{[n]!} \tag{6}$$

is

$(z-z^*)^0 = 1,\ (z-z^*) = \prod_{j=0}^{n-1}(z-qz^*)^j,$ for $n \in \mathbb{N}$,

and $D_q, D_q^{(2)}, D_q^{(3)}, \ldots$ are the q-derivatives.

Moreover, the rest of the manuscript is designed as follows: In section 2, we have shown the basic definition, order of convergence, and scaling theorem for the proposed method. Section 3 is devoted to the complex dynamics of the Quantum iterative method, with a brief discussion of its fixed and critical points. The dynamical plane of the method using a cubic polynomial has also been discussed in this section. In Section 4, the real dynamics of the proposed method using some real-world problems are discussed. Finally, section 5 ends with the conclusion.

2 Parametric family of Quantum iterative method (PFQIM) and its convergence analysis

To solve equation (1) iteratively, we introduce a parametric family of quantum iterative methods (PFQIM) defined as follows:

$$\begin{cases} z_0 \text{ given}, \\ z_{k+1} = Q_{S,\delta,q}(z_k) = z_k - \left(1 + \frac{0.5L_S(z_k)}{(1-\delta * L_S(z_k))}\right)\frac{S(z_k)}{D_qS(z_k)}, \end{cases} \tag{7}$$

where $L_S(z_k) = \frac{S(z_k)D_q^{(2)}S(z_k)}{(D_qS(z_k))^2}$ and $\delta \in \mathbb{C}$ is the complex parameter.

Theorem 1. Let $S(z)$ be an analytic function, and let $T(z) = \alpha z + \beta$, with $\alpha \neq 0$, be an affine map. Suppose $f(z) = \rho(S \circ T)(z)$, where ρ is a nonnull constant. Then $(T \circ Q_{S,\delta,q} \circ T^{-1})(z) = Q_{f,\delta,q}(z)$, that is, $Q_{S,\delta,q}$ and $Q_{f,\delta,q}$ are affine conjugate through T.

Proof. First, we have $T^{-1}(z) = \frac{1}{\alpha}(z-\beta)$. Moreover,

$$\begin{aligned} Q_{S,\delta,q} \circ T^{-1}(z) &= Q_{S,\delta,q}(T^{-1}(z)) \\ &= T^{-1}(z) - \left(1 + \frac{0.5L_S(T^{-1}(z))}{(1-\delta L_S(T^{-1}(z)))}\right)\frac{S(T^{-1}(z))}{D_qS(T^{-1}(z))}. \end{aligned}$$

On the other side, as $f \circ T^{-1}(z) = S(z)$,

$$D_q(f\circ T^{-1})(z)=\frac{1}{\alpha}D_qf(T^{-1}(z))$$

and

$$D_q^{(2)}(f\circ T^{-1})(z)=\frac{1}{\alpha^2}D_q^{(2)}f(T^{-1}(z)).$$

From the above, $D_qf(T^{-1}(z))=\alpha D_qS(z)$ and $D_q^{(2)}f(T^{-1}(z))=\alpha^2D_q^{(2)}S(z)$. So we have $L_f(T^{-1}(z))=L_S(z)$ and $\frac{S(T^{-1}(z))}{D_qS(T^{-1}(z))}=\frac{1}{\alpha}\frac{f(z)}{D_qf(z)}$. Now, by substituting these expressions and using the definition of $Q_{S,\delta,q}\circ T^{-1}(z)$, we have

$$\begin{aligned}T\circ Q_{S,\delta,q}\circ T^{-1}(z)&=T(Q_{S,\delta,q}(T^{-1}(z)))\\&=\alpha.Q_{S,\delta,q}(T^{-1}(z))+\beta\\&=\alpha.\left[T^{-1}(z)-\left(1+\frac{0.5L_S(T^{-1}(z))}{(1-\delta L_S(T^{-1}(z)))}\right)\frac{S(T^{-1}(z))}{D_qS(T^{-1}(z))}\right]\\&\quad+\beta\\&=z-\left(1+\frac{0.5L_f(z)}{(1-\delta L_f(z))}\right)\frac{f(z)}{D_qf(z)}=Q_{f,\delta,q}.\end{aligned}$$

□

The scaling theorem enables the study of iterative methods through simpler function families after an appropriate coordinate transformation.

Now, we have presented the order of convergence of the proposed method in the next theorem.

Theorem 2. Let $S:D\subseteq\mathbb{C}\to\mathbb{C}$ be a q-differentiable function in the open disk $D\subseteq\mathbb{C}$. If $S(z)=0$ has a simple root $z^*\in D$ and z_0 is the initial guess sufficiently close to z^*, then the above method defined in (7) has cubic order convergence denoted as $[3;q]$, where q indicates the q-derivative, and the error equation of the proposed method is given below:

$$e_{k+1}=(2P_2^2-P_3-2\delta P_2^2)e_k^3+O(e_k^4). \tag{8}$$

Proof. The q-Taylor series of $S(z_k)$ and its first order q-derivative are

$$S(z_k)=D_qS(z^*)(e_k+P_2e_k^2+P_3e_k^3)+O(e_k^4), \tag{9}$$

$$D_q(z_k)=D_qS(z^*)(1+2P_2e_k+3P_3e_k^2)+O(e_k^3), \tag{10}$$

where $e_k=z_k-z^*$ and $P_n=\frac{D_q^{(n)}S(z^*)}{[n]!D_qS(z^*)}$, $n=2,3,\ldots$. The second order q-derivative of q-Taylor's series can be given as

$$D_q^{(2)}S(z_k)=D_qS(z^*)(2P_2+6P_3e_k)+O(e_k^2). \tag{11}$$

From (9) and (10), we have

$$\frac{S(z_k)}{D_q S(z_k)} = e_k - P_2 e_k^2 - (2P_3 - 2P_2^2)e_k^3 + O(e_k^4)$$

and

$$L_S(z_k) = \frac{S(z_k) D_q^{(2)} S(z_k)}{(D_q S(z_k))^2} = 2P_2 e_k + (6P_3 - 6P_2^2)e_k^2 + (16P_2^3 - 28P_2P_3)e_k^3 + O(e_k^4).$$

Next, using (12) and (2) implies

$$\left(1 + \frac{0.5L_S(T^{-1}(z))}{(1 - \delta L_S(T^{-1}(z)))}\right)\frac{S(z_k)}{D_q S(z_k)} = e_k + (2P_2^2 - P_3 - 2\delta P_2^2)e_k^3 + O(e_k^4). \tag{12}$$

Finally, substituting (12) into (7), and simplifying a little, the desired error equation will be

$$e_{k+1} = (2P_2^2 - P_3 - 2\delta P_2^2)e_k^3 + O(e_k^4).$$

□

Lemma 1. With the local error equation is given in (8) of Theorem 2, we define the asymptotic error constant as

$$K(\delta) = 2P_2^2 - P_3 - 2\delta P_2^2. \tag{13}$$

The term $K(\delta)$ linearly dependent on the parameter δ, and therefore the parameter can be chosen to minimize or even annihilate this coefficient, so we have the following special case.

Optimal choice of δ.

Setting $K(\delta) = 0$ gives

$$\delta^\star = \frac{2P_2^2 - P_3}{2P_2^2} = 1 - \frac{P_3}{2P_2^2}, \qquad (P_2 \neq 0).$$

If $\delta = \delta^\star$, then the cubic term vanishes and the error equation becomes

$$e_{k+1} = O(e_k^4),$$

indicating that the rate of convergence increases from cubic to at least quartic. Hence, $\delta^\star$ gives the optimal value minimizing the asymptotic error constant $|K(\delta)|$.

3 Complex dynamics PFQIM

It is required to recall some basic dynamical ideas in order to understand the dynamical behavior of an iterative method when applied to a polynomial $S(z)$. Let $R : \mathbb{C}^* \to \mathbb{C}^*$ be the rational function defined on the Riemann sphere. Then the orbit of a point $z_0 \in \mathbb{C}^*$ is the set of composition functions by $\{z_0, R(z_0), R^2(z_0), \ldots, R^n(z_0), \ldots\}$. A point $z_0 \in \mathbb{C}^*$ is a fixed point of R if $R(z_0) = z_0$, and the behavior of fixed points is attracting, repelling, or neutral if $|D_q R(z_0)| \leq d < 1$, $|D_q R(z_0)| > 1$ or $|D_q R(z_0)| = 1$, respectively. Moreover, if $|D_q R(z_0)| = 0$, then the fixed points are called as super attracting.

The fixed points that do not belong to the roots z^* of $S(z)$ are called strange fixed points. If z^* is an attracting fixed point, then the basin of attraction of the fixed point is the set of preimages $\mathcal{A}(z^*) = \{z_0 \in \mathbb{C}^* : R^n(z_0) \to z^*, n \to \infty\}$. The Fatou set, $\mathcal{F}(R)$, is the set of points whose orbits tend to an attractive fixed point z^*. The complement of $\mathcal{F}(R)$ is the Julia set $\mathcal{J}(R)$ that consists of the repelling fixed points.

We now apply PFQIM (7) to a quadratic polynomial $S(z) = z^2 - a$, where $a \in \mathbb{C}^*$ and the Möbius transformation $\mathcal{M}(z) = \frac{z-a}{z+a}$ with the inverse $[\mathcal{M}(z)]^{-1} = \frac{-a(z+1)}{z-1}$ to produce the rational map relating to the quantum iterative method (7) as follows:

$$\begin{aligned} &Q_{\mathcal{M}}(z,\delta,q) \\ &= \frac{z(-1+q^2-5z+2qz+3q^2z+z^2+4qz^2+3q^2z^2+z^3+2qz^3+q^2z^3+4z\delta-4qz\delta-4z^2\delta-4qz^2\delta)}{1+2q+q^2+z+4qz+3q^2z-5z^2+2qz^2+3q^2z^2-z^3+q^2z^3-4z\delta-4qz\delta+4z^2\delta-4qz^2\delta}. \end{aligned}$$

Also, the operator obtained from the quantum Newton method when $\delta \to \infty$ is

$$Q_{\mathcal{NM}}(z,\delta,q) = \frac{z(q+z+qz-1)}{q-z+qz+1}.$$

3.1 Study of fixed points and their stability

The fixed and strange fixed points of the rational operator $Q_{\mathcal{M}}(z,\delta,q)$ are obtained by solving the equation $Q_{\mathcal{M}}(z,\delta,q) = z$. Note that $z = 0$, $z = 1$ and $z = \infty$ are fixed points of $Q_{\mathcal{M}}(z,\delta,q)$ out of which the fixed points $z = 0$ and $z = \infty$ are super-attracting. The strange fixed points are

$z = \frac{2\delta - \sqrt{4\delta^2-8\delta-4\delta q+2q+3}-q-2}{q+1}$ and $z = \frac{2\delta + \sqrt{4\delta^2-8\delta-4\delta q+2q+3}-q-2}{q+1}$.

Next, we observe that the parameter δ affects not only the number of fixed points but also their stability. The q-derivative rational operator expression, which is required for studying the stability of fixed points and determining critical points, is

$$\begin{aligned}D_qQ_{\mathcal{M}}(z,\delta,q) =& -\frac{1}{(q-1)}\Big[q^2z^3+3q^2z^2+3q^2z+q^2+2qz^3-4\delta qz^2+4qz^2\\
&-4\delta qz+2qz+z^3-4\delta z^2+z^2+4\delta z5z-1\Big]\frac{1}{z(q-1)}\\
&\Big[(q^5z^3+3q^4z^2-q^3z^3-4\delta q^3z^2+2q^3z^2+3q^3z-q^2z^3\\
&+4\delta q^2z^2)+(-8q^2z^2-4\delta q^2z+q^2z+4\delta qz^2-2qz^2-3qz\\
&+z^3-4\delta z^2+5z^2+4\delta z-z)-(q^2z^3+3q^2z^2+3q^2z+q^2\\
&-4\delta qz^2+2qz^2-4\delta qz+4qz+2q-z^3+4\delta z^2-5z^2)\\
&-\frac{(4\delta z+z+1)}{(q-1)z}\Big(z(q^2z^3+3q^2z^2+3q^2z+q^2+2qz^3-4\delta qz^2\\
&+4qz^2-4\delta qz+2qz+z^3-4\delta z^2+z^2+4\delta z-5z-1)\\
&-qz(q^5z^3+2q^4z^3+3q^4z^2+q^3z^3-4\delta q^3z^2+4q^3z^2+3q^3z\\
&-4\delta q^2z^2+q^2z^2-4\delta q^2z+2q^2z+q^2+4\delta qz-5qz-1)\Big)\Big].\end{aligned}$$

Table 1 presents the critical points of the operators for different values of δ and q.

Table 1: Critical points of operators $Q_{\mathcal{M}}(z,\delta,q)$ and $Q_{\mathcal{NM}}(z,\delta,q)$(when $\delta=\infty$) for δ and $q=0.1,\ 0.5,$ and 0.999

q, δ	Critical points
$q=0.1$, $\delta=0$	-53.691, -3.721, -2.687, -0.186, 1.834, 5.451
$q=0.1$, $\delta=0.5$	27.998, -10, -1, -0.357, 2.864, 3.490
$q=0.1$, $\delta=1$	-9.229-17.935i, -9.229+17.935i, -0.226-0.440i, -0.226+0.440i, 2.955-1.123i, 2.955+1.123i
$q=0.1$, $\delta=\infty$	0, 0.7903, 12.6542
$q=0.5$, $\delta=0$	-13.806, -1.391-0.252i, -1.391+0.252i, -0.144, 0.647, 3.086
$q=0.5$, $\delta=0.5$	-8.772, -2, -1, -0.227, 1, 2
$q=0.5$, $\delta=1$	-4.665-1.082i, -4.665+1.082i, -0.406-0.0943i, -0.406+ 0.094i, 1.372-0.340i, 1.372+ 0.340i
$q=0.5$, $\delta=\infty$	0, 0.2280, 8.7720
$q=0.999$, $\delta=0$	-15.071, -1.053-0.031i, -1.053+0.031i, -0.073, 0.129, 8.566
$q=0.999$, $\delta=0.5$	-10.396, -1.111, -1, -0.106, 0.182, 6.098
$q=0.999$, $\delta=1$	-3.559-4.271i, -3.559+4.271i, -0.127-0.153i, -0.127+0.153i, 0.385, 2.878
$q=0.999$, $\delta=\infty$	0, 2.5025e-04, 4.0000e+03

The dynamical graphs of the proposed method in this paper are plotted with a mesh of 1500×1500 real points using a Lenovo Ideapad flex 5, 1.19 GHz, Intel(R) Core(TM) i5-1035G1 CPU. The stopping criteria of the convergence plane have a tolerance of 10^{-3} and a maximum of

20 iterations. We have represented the convergence basins of each iterative procedure using the MATLAB program described in [5]. If the iterative method converges to the fixed point zero, then it is painted in cyan, and for ∞, it is painted in magenta, and if no root is found with a maximum of 20 iterations, the dynamical plane is painted in black. The attracting fixed points are marked in the figures by white stars, the parabolic fixed points by white circles, and the critical points by white squares. When the number of iterations decreases, the color will be more intense. If the method reaches the maximum number of iterations, then the point will become black.

We have plotted the dynamical planes of PFQIM for different values of δ with different values of q, such as $q = 0.5$ and $q = 0.999$. It can be observed that when the value of q is close to 1, the parametric plane is stable, excluding the boundary of the Fatou set. The star marks and square marks are denoted as the fixed and critical points, while circle points are taken as the parabolic points of the corresponding operator $Q_{\mathcal{M}}(z, \delta, q)$.

In particular, Figure 1 shows that in case (a), the method is stable with more fixed points, critical points, and iterations; in case (b), the number of fixed and critical points are reduced, and the Julia set is connected in the circumference; in case (c), the method is stable with more Julia sets; $z = 0$ is the repelling fixed point, and an orbit with 20 iterations is shown; and in case (d), the method is stable, but there are no Julia sets. In Figure 2, the dynamical planes are brighter than the previous one, meaning the method requires fewer iterations to converge on a root. In Figure 3, the stable behavior of a fixed point is seen at $q = 0.999$ and $\delta = 3.9 + 0.1i$, surrounding a complicated Julia set.

3.2 Dynamics plane on cubic polynomials

In this part, we have represented some dynamical planes of cubic polynomials when applied to PFQIM. Figure 4 illustrates the behavior of the family (7) on the cubic polynomial $z^3 - 1$. For different values of δ, we have called iterative methods like the Quantum Newton method (QNM, for $\delta = \infty$), Quantum Chebyshev method (QCM, for $\delta = 0$), Quantum Halley method (QHM, for $\delta = 0.5$), and the Quantum super-Halley method (QSCM, for $\delta = 1$). In Figure 4: (a), (b), (c), and (d), the dynamical planes of PFQIM are shown for $q = 0.5$, where the iterative family of method's behavior is unstable; in Figure 4: (e), (f), (g), and (h), the basin of attraction towards the divergent region is reduced, and the more stable zone is obtained; the intensity of the color is more intense, i.e., the convergence is faster. Moreover, the percentage of convergence of each dynamic plane is given in the figures, which gives an idea of the stability of the methods.

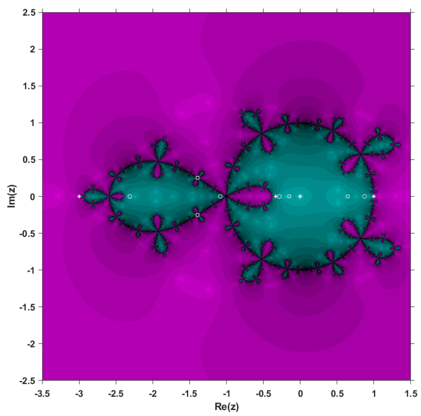

(a) PFQIM; $q = 0.5$, $\delta = 0$

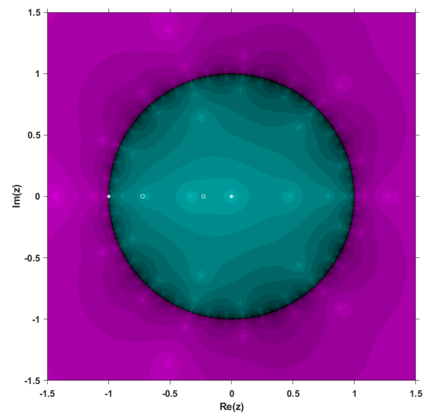

(b) PFQIM; $q = 0.5$, $\delta = 0.5$

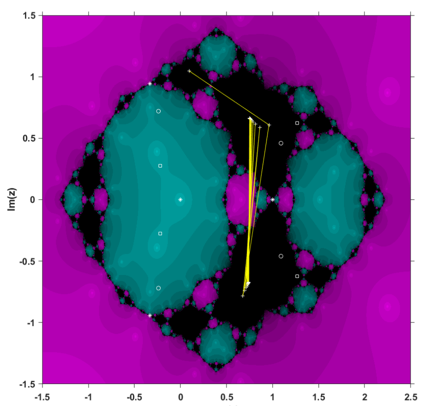

(c) PFQIM; $q = 0.5$, $\delta = 1$

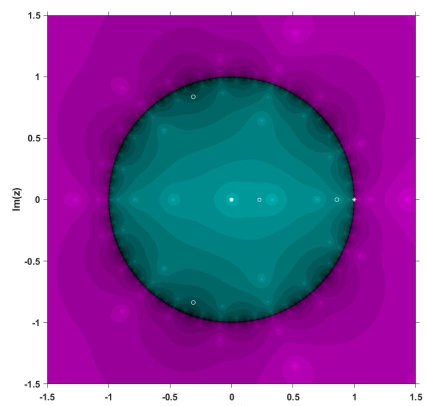

(d) QNM; $q = 0.5$, $\delta = \infty$

Figure 1: Dynamical planes of $Q_{\mathcal{M}}(z, \delta, q)$ and $Q_{\mathcal{NM}}(z, \delta, q)$

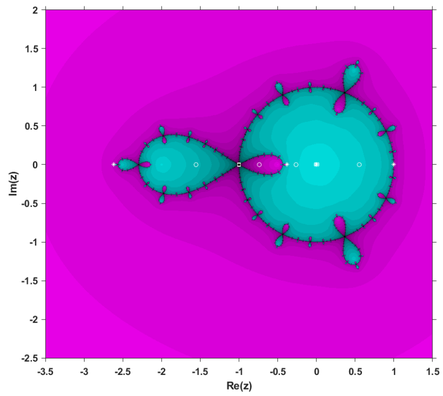

(a) PFQIM; $q = 0.999$, $\delta = 0$

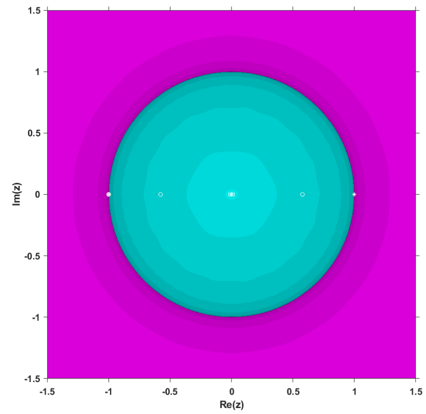

(b) PFQIM; $q = 0.999$, $\delta = 0.5$

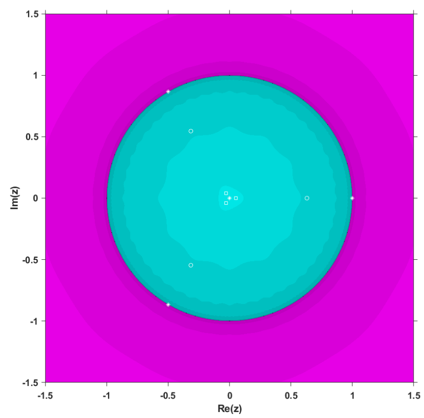

(c) PFQIM; $q = 0.999$, $\delta = 1$

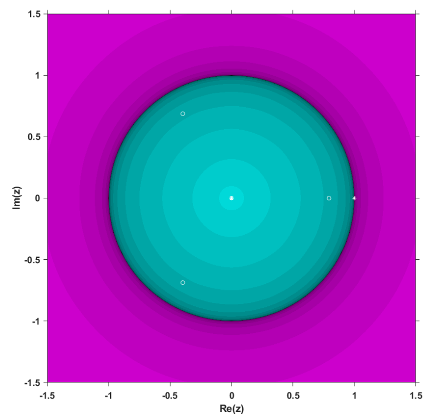

(d) QNM; $q = 0.999$, $\delta = \infty$

Figure 2: Dynamical planes of $Q_{\mathcal{M}}(z, \delta, q)$ and $Q_{\mathcal{NM}}(z, \delta, q)$

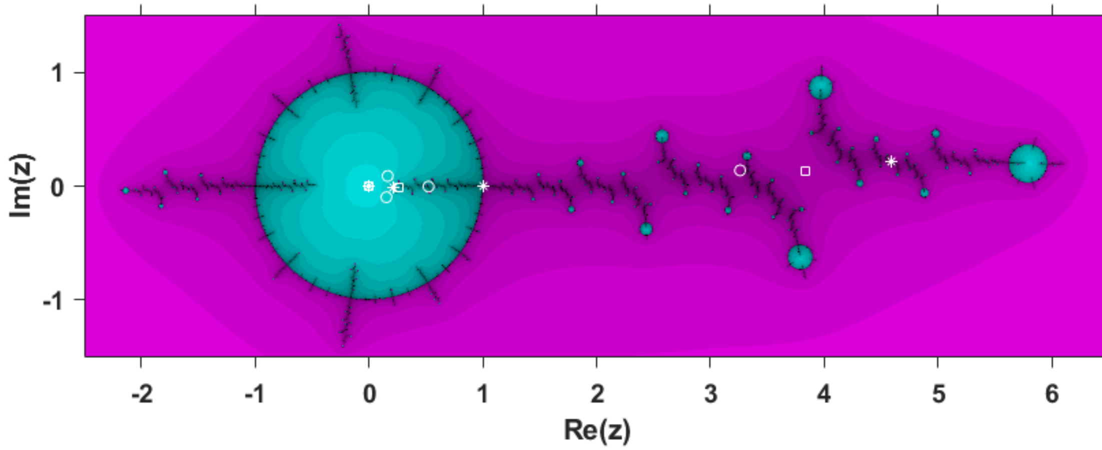

Figure 3: Dynamical plane of operator at $q = 0.999$ and $\delta = 3.9 + 0.1i$

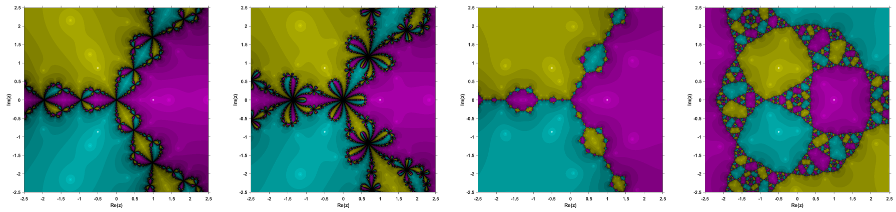

(a) QNM, $q = 0.7$, 98.69% convergence
(b) QCM, $q = 0.7$, 96.83% convergence
(c) QHM, $q = 0.7$, 99.99% convergence
(d) QSHM, $q = 0.7$, 99.83% convergence

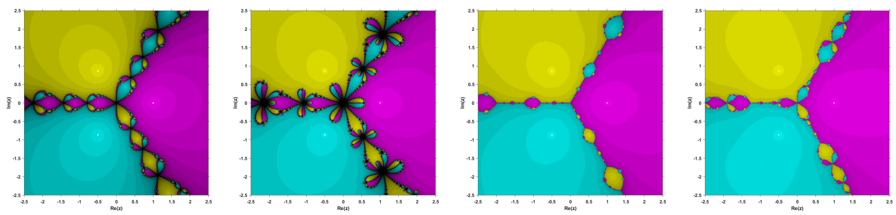

(e) QNM, $q = 0.999$, 99.53% convergence
(f) QCM, $q = 0.999$, 98.55% convergence
(g) QHM, $q = 0.999$, 99.99% convergence
(h) QSHM, $q = 0.999$, 100% convergence

Figure 4: Dynamic planes of cubic polynomial $z^3 - 1$ on PFQIM

4 Real dynamics of PFQIM

In this part, we have visualized the real dynamics (for more details readers can see the articles, [14, 13]) of the proposed method using some real-world applications. Here, the value of the q-derivative is taken as $q \in (0, 2]$. Additionally, the approximate computational order of convergence ($ACOC$) [6], is used to confirm that the theoretical order of convergence is also obtained in practice for single variable equations, can be calculated by the formula given below:

$$ACOC = \frac{\ln |(x_{k+1} - x_k|/|x_k - x_{k-1}|)}{\ln(|x_k - x_{k-1}|/|x_{k-1} - x_{k-2}|)}, \qquad k = 2, 3, 4, \ldots.$$

In the numerical table, we have shown the root of the equation, error, functional value at the nth iteration, ACOC, and CPU time in seconds. The convergence planes are potted using Matlab R2022b by modifying the program made in [12]. The term stable points refers to the collection of all starting points for which the iterative process generates a convergence region. Initial guesses and the parameter q both play a major role in determining whether iterative methods are stable. We illustrate the stability and dynamical properties of the method using convergence planes.

4.1 Numerical results

Example 4.1 (Kepler's laws of planetary motion)**.** In astronomy, Kepler's laws of planetary motion [17] are used to locate the position of a planet in the elliptical path that moving around the Sun. Kepler's equation applies to the motion of any object in an elliptical orbit. For example, Earth or Mars orbits around the Sun, or any moon orbiting a planet, or a rocket or satellite in orbit about any planet or moon. So our first test example is Kepler's equation, which can be written as $S_1(x) = x - e\sin(x) - M$, where $M$is the mean anomaly and e is the eccentricity of an object in an elliptical orbit. Suppose $M = \frac{\pi}{6}$ and $e = 0.6$; then the equation reduces to $S_1(x) = x - 0.6\ \sin(x) - \frac{\pi}{6}$ with root $x = 1.04149$. The numerical tables contain q as the order of derivative, and x^* is the approximate root. Tables 2, 3, 5, and 6 show that the speed of convergence increases as the value of q approaches one. Furthermore, in Tables 4 and 7, the numerical results of corresponding classical iterative are presented (for initial guesses $x_0 = 2$ and $x_0 = 2.5$), where we can observed that PFQIM for different values of $q = 0.999$, $q = 0.999999$, and $q = 0.9999999$ performf quite similar to classical methods, although in some cases it show slightly variations in the $ACOC$.

Table 2: Results of QSHM, QHM for $S_1(x)$ with initial guess $x_0 = 2$

	QSHM						QHM					
q	x^*	$\lvert x_{k+1} - x_k\rvert$	$\lvert S_1(x_{k+1})\rvert$	ACOC	CPU	Iter	x^*	$\lvert x_{k+1} - x_k\rvert$	$\lvert S_1(x_{k+1})\rvert$	ACOC	CPU	Iter
0.7	x_1	5.41206e-06	4.0778e-07	1.01	0.05	07	x_1	3.39205e-06	2.55579e-07	1.0	0.51	07
0.8	x_1	5.024231e-06	2.590377e-07	0.99	0.06	06	x_1	2.434003e-06	1.254917e-07	0.99	0.49	06
0.999	x_1	1.56993e-05	4.23311e-09	2.3	0.04	03	x_1	4.42721e-06	1.19374e-09	3.7	0.057	03
0.999999	x_1	2.934109e-06	7.91589e-13	2.84	0.076	03	x_1	2.39488e-05	6.42819e-12	3.11	0.069	03
0.9999999	x_1	2.03524e-05	1.18538e-12	2.22	0.074	03	x_1	2.65808e-05	9.35374e-12	3.06	0.066	03

Table 3: Results of QCM, QNM for $S_1(x)$ with initial guess $x_0 = 2$

	QCM						QNM					
q	x^*	$\lvert x_{k+1} - x_k\rvert$	$\lvert S_1(x_{k+1})\rvert$	ACOC	CPU	Iter	x^*	$\lvert x_{k+1} - x_k\rvert$	$\lvert S_1(x_{k+1})\rvert$	ACOC	CPU	Iter
0.7	x_1	2.22229e-06	1.674418e-07	1.0	0.05	07	x_1	2.15963e-06	1.62721e-07	1.0	0.04	07
0.8	x_1	1.04465e-05	5.38613e-07	1.0	0.04	05	x_1	2.78538e-06	1.43606e-07	0.99	0.04	06
0.999	x_1	1.16708e-04	3.14705e-08	2.9	0.05	03	x_1	8.202927e-05	2.03785e-08	2.04	0.05	04
0.999999	x_1	1.5812e-04	4.2838e-11	2.84	0.074	03	x_1	8.9510e-05	2.0506e-09	2.02	0.78	04
0.9999999	x_1	1.4927e-04	9.0351e-11	2.86	0.65	03	x_1	8.9517e-05	2.0726e-09	2.02	0.65	04

Table 4: Results of classical SHM, HM, CM, and NM for $S_1(x)$ with initial guess $x_0 = 2$

Methods	x^*	$\lvert x_{k+1} - x_k\rvert$	$\lvert S_1(x_{k+1})\rvert$	ACOC	CPU	Iter
SHM	x_1	2.7000004e-06	1.11022302e-16	2.85	0.045	03
HM	x_1	2.363779e-05	6.661338e-16	3.12	0.045	03
CM	x_1	1.5668661e-04	5.4578563e-13	2.85	0.045	03
NM	x_1	8.95180e-05	2.075144e-09	2.02	0.07	04

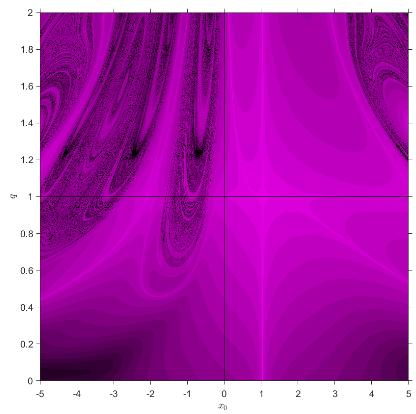

(a) QSHM, 99.16%

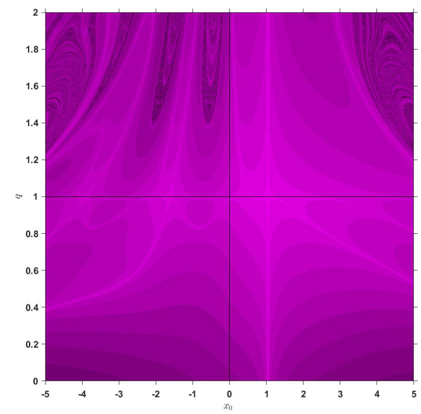

(b) QHM, 99.79%

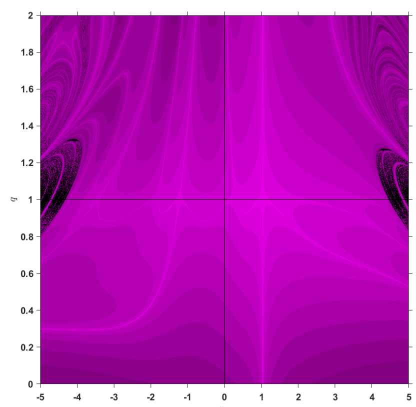

(c) QCM, 98.81%

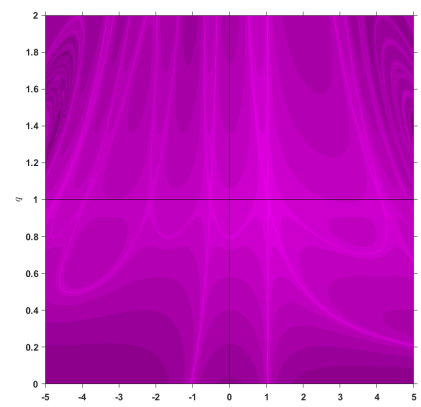

(d) QNM, 99.86%

Figure 5: Convergence planes of $S_1(x)$, $x_0 \in \mathbb{R}$

Table 5: Results of QSHM, QHM for $S_1(x)$ with initial guess $x_0 = 2.5$

	QSHM							QHM					
q	x^*	$\lvert x_{k+1}-x_k\rvert$	$\lvert S_1(x_{k+1})\rvert$	ACOC	CPU	Iter	x^*	$\lvert x_{k+1}-x_k\rvert$	$\lvert S_1(x_{k+1})\rvert$	ACOC	CPU	Iter
0.7	x_1	8.043468e-06	6.06048e-07	1.00	0.067	07	x_1	3.79807e-06	2.86172e-07	1.0	0.71	07
0.8	x_1	5.309870e-06	2.737646e-07	0.99	0.066	06	x_1	1.145934e-05	5.90820e-07	1.00	0.66	05
0.999	x_1	2.99318e-04	8.06974e-08	3.11	0.057	03	x_1	5.40366e-04	1.45734e-07	3.18	0.064	03
0.999999	x_1	2.2857e-04	6.17301e-11	3.25	0.058	03	x_1	6.36395e-04	1.01844e-10	3.11	0.063	03
0.9999999	x_1	3.62815e-04	5.76748e-10	3.044	0.063	03	x_1	5.61367e-04	4.05469e-09	3.19	0.061	03

Table 6: Results of QCM, QNM for $S_1(x)$ with initial guess $x_0 = 2.5$

	QCM							QNM					
q	x^*	$\lvert x_{k+1}-x_k\rvert$	$\lvert S_1(x_{k+1})\rvert$	ACOC	CPU	Iter	x^*	$\lvert x_{k+1}-x_k\rvert$	$\lvert S_1(x_{k+1})\rvert$	ACOC	CPU	Iter
0.7	x_1	1.32199e-05	9.96074e-07	0.99	0.066	06	x_1	2.15963e-06	1.62721e-07	1.0	0.04	07
0.8	x_1	1.8032e-06	9.29707e-08	1.00	0.070	06	x_1	2.78538e-06	1.43606e-07	0.99	0.04	06
0.999	x_1	0.00189	5.106281e-07	2.74	0.060	03	x_1	6.41092e-04	6.6580e-08	2.04	0.054	04
0.999999	x_1	0.00223	5.54425e-09	2.66	0.062	03	x_1	6.64269e-04	1.1411e-07	2.02	0.062	04
0.9999999	x_1	0.00201	3.7527e-10	2.71	0.062	03	x_1	6.6429e-04	1.1428e-07	2.02	0.055	04

Table 7: Results of classical SHM, HM, CM, and NM for $S_1(x)$ with initial guess $x_0 = 2.5$

Methods	x^*	$\lvert x_{k+1}-x_k\rvert$	$\lvert S_1(x_{k+1})\rvert$	ACOC	CPU	Iter
SHM	x_1	2.32205e-04	6.32383e-13	3.25	0.065	03
HM	x_1	6.362408e-04	1.17829e-11	3.11	0.062	03
CM	x_1	0.00201	1.158377e-09	2.71	0.059	03
NM	x_1	6.64292e-04	1.142994e-07	2.029	0.054	04

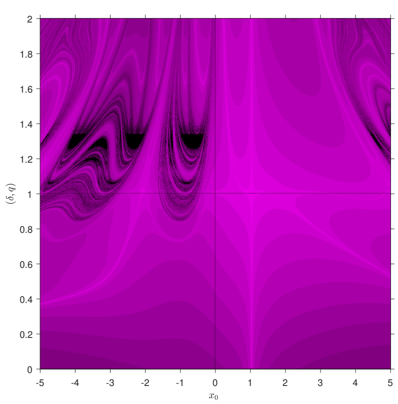

(a) PFQIM, for parameters (δ, q), 95.72%

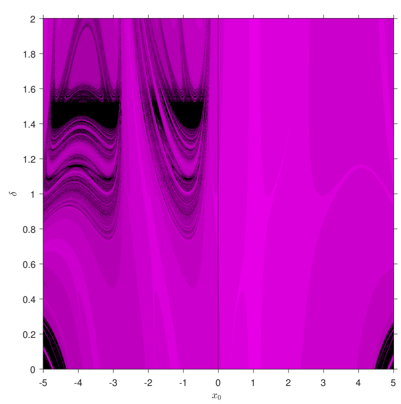

(b) PFQIM, for parameters (δ), 95.36%

Figure 6: Convergence planes of $S_1(x)$ for different parameters

The convergence plane of each iterative method and its percentage of convergence are described in Figure 5. The root x_1 is painted in the magenta color and the faster convergence of the method reaches the root is brighter in the convergence plane. As given in the figure, QSHM (99.16%), QHM (99.79%), QCM (98.81%), and QNM (99.86%) among which the cubic order convergence method gives faster convergence then QNM. It can be also observed that at the order of derivative $q = 1$, the method is not converging to the root. Although the qualitative behavior of the proposed method on S_1 is illustrated for different parameters in Figure 6

(a) shows the combination of parameters pairs (δ, q) along $y - axis$, while Figure 6 (b) represents the variation of the parameter δ at $q = 0.999$ to study the stability of method in depth way.

Our second test function is the polynomial obtained from the Schrödinger wave equation, which is given in the example below.

Example 4.2 (Schrödinger wave equation for a hydrogen atom)**.** In quantum physics, the solution of the Schrödinger wave equation [19] for a charged particle moving in a Coulomb potential is linked to a probability distribution for the electron's location relative to the core. The standard Schrödinger equation for a particle with mass m traveling in a central potential is given by

$$-\frac{\hbar^2}{2m}\frac{\partial \Phi}{\partial t} - K\frac{e^2}{r}\Phi = E\Phi,$$

where r is the distance of the electron from the core and E is the energy. Also, the equation has the following representation in spherical coordinates:

$$-\frac{\hbar^2}{2m}\left[\frac{1}{r^2}\frac{\partial(r^2\frac{\partial\Phi}{\partial r})}{\partial r} + \frac{1}{r^2\sin\theta}\frac{\partial(\sin\theta\frac{\partial\Phi}{\partial\theta})}{\partial\theta} + \frac{1}{r^2\sin^2\theta}\frac{\partial^2\Phi}{\partial\psi^2}\right] + \frac{e^2\Phi}{r} = E\Phi.$$

The standard technique can be used to separate the final equation into angular and radial parts. The angular equation can also be written as a system of two equations, one of which is the Legendre equation [3].

$$(1-x^2)\frac{d^2g}{dx^2} - 2x\frac{dg}{dx} + \left(n(n+1) - \frac{m^2}{1-x^2}\right)g(x) = 0.$$

The equation is simplified to Legendre polynomials when $m = 0$, corresponding to the azimuthal symmetry situation. We use the following form of the Legendre equation that we have derived:

$$S_2(x) = 46189x^{10} - 109395x^8 + 90090x^6 - 30030x^4 + 3465x^2 - 63$$

with the roots, $x_1 = -0.9739$ (cyan), $x_2 = 0.9739$ (magenta), $x_3 = -0.8651$ (yellow), $x_4 = 0.8651$ (red), $x_5 = -0.6794$ (green), $x_6 = 0.6794$ (blue), $x_7 = -0.4334$ (white), $x_8 = 0.4334$ (dark red), $x_9 = -0.1489$ (dark green), and $x_{10} = 0.1489$ (dark blue) are painted in the respective colors given in Figure 7.

Moreover, the numerical results of $S_2(x)$ are shown in Tables 8 and 9 and compared with corresponding classical methods as given in Table 10, where "dgt" denotes divergence and "–" in *ACOC* denotes an extremely large or undefined value.

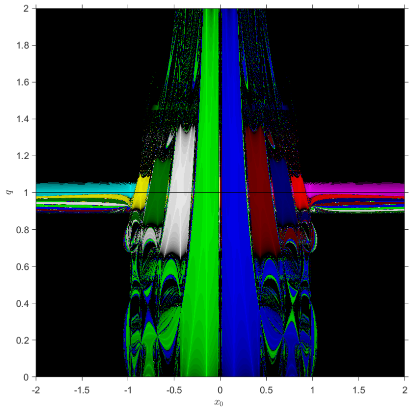

(a) QSHM, 34.95%

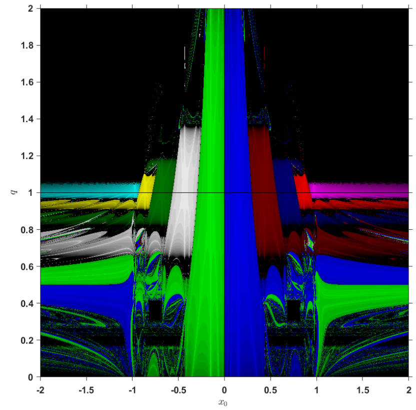

(b) QHM, 52.44%

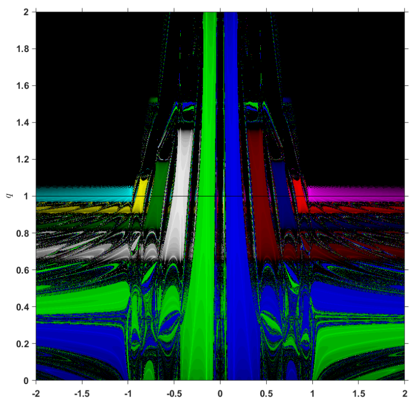

(c) QCM, 49.43%

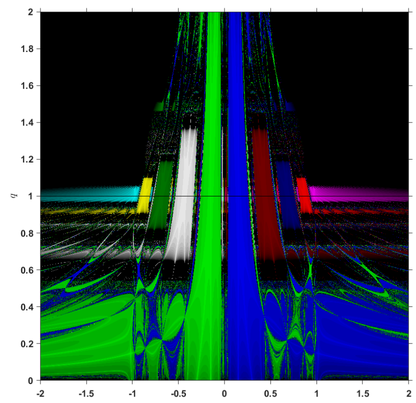

(d) QNM, 51.63%

Figure 7: Convergence planes of $S_2(x)$, $x_0 \in \mathbb{R}$

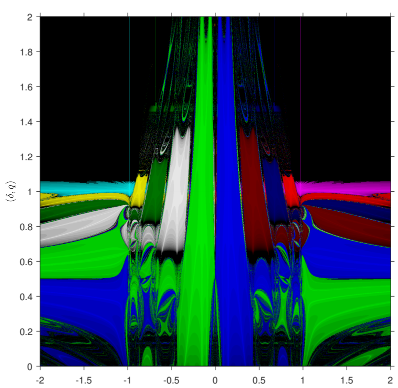

(a) PFQIM,, for parameters (δ, q) 55.13%

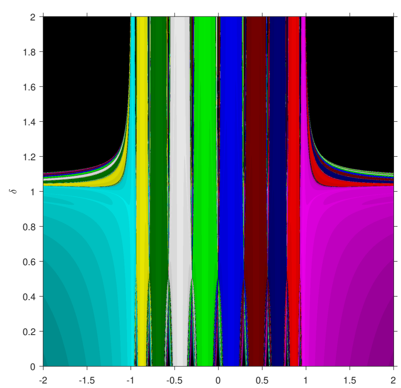

(b) PFQIM, for parameters (δ), 77.58%

Figure 8: Convergence planes of $S_2(x)$ for different parameters

Table 8: Results of QSHM, QHM for $S_2(x)$ with initial guess $x_0 = 1.5$

	QSHM						QHM					
q	x^*	$\lvert x_{k+1} - z_k\rvert$	$\lvert S_1(x_{k+1})\rvert$	ACOC	CPU	Iter	x^*	$\lvert x_{k+1} - x_k\rvert$	$\lvert S_1(x_{k+1})\rvert$	ACOC	CPU	Iter
0.7	x_8	5.75570e-07	1.61295e-04	1.0	0.08	21	x_8	5.7557e-07	1.61295e-04	1.0	0.05	21
0.8	dgt	0.03984	27.29704	–	0.05	500	dgt	0.03984	27.29704	–	0.05	500
0.999	x_2	5.0865e-08	5.74888e-06	0.7	0.06	04	x_2	5.08650e-08	5.74888e-06	0.7	0.05	12
0.999999	x_2	9.192652e-07	1.04597e-07	2.47	0.074	04	x_2	1.483287e-07	1.68633e-08	2.91	0.096	07
0.9999999	x_2	6.8850e-08	7.6988e-10	3.18	0.093	04	x_2	1.0325e-07	1.1996e-09	3.01	0.093	07

Table 9: Results of QCM, QNM for $S_2(x)$ with initial guess $x_0 = 1.5$

	QCM						QNM					
q	x^*	$\lvert x_{k+1} - x_k\rvert$	$\lvert S_1(x_{k+1})\rvert$	ACOC	CPU	Iter	x^*	$\lvert x_{k+1} - z_k\rvert$	$\lvert S_1(x_{k+1})\rvert$	ACOC	CPU	Iter
0.7	x_8	6.49974e-07	1.82144e-04	1.0	0.04	27	x_8	5.755708e-07	1.61295e-04	1.0	0.04	21
0.8	dgt	2.34549e-07	3.44064e-05	1.0	0.05	500	dgt	0.03984	27.29704	–	0.05	500
0.999	x_2	5.08650e-08	5.74888e-06	0.9	0.05	12	x_2	1.030859e-08	1.16369e-09	2.01	0.069	12
0.999999	x_2	2.10233e-06	2.3916e-07	2.79	0.063	08	x_2	1.03085e-08	1.16369e-09	2.01	0.064	12
0.9999999	x_2	2.05854e-06	1.913076e-08	2.81	0.073	08	x_2	1.07319e-08	1.15505e-10	2.00	0.066	12

Table 10: Results of classical SHM, HM, CM, and NM for $S_2(x)$ with initial guess $x_0 = 1.5$

Methods	x^*	$\lvert x_{k+1} - x_k\rvert$	$\lvert S_1(x_{k+1})\rvert$	ACOC	CPU	Iter
SHM	x_2	8.8108443e-07	3.63797880e-12	2.48	0.067	04
HM	x_2	1.63192236e-07	1.6825651e-11	2.87	0.07	07
CM	x_2	2.12884862e-06	4.2291503e-11	2.79	0.064	08
NM	x_2	1.0779137e-08	1.9554136e-11	2.00	0.046	12

The convergence planes of S_2 are illustrated in Figure 7, where distinct colors represent different roots of the polynomial, excluding black. The qualitative performance of the proposed method on S_2 is analyzed under different parameter choices. Figure 8 (a) displays the combinations of (δ, q) along the y-axis, while Figure 8 (b) illustrates how varying δ at $q = 0.999$ helps explore the stability of the method in greater detail.

5 Conclusion

We studied the complex and real dynamics of a newly designed Chebyshev–Halley family iterative method using the q-derivative. We proved a scaling theorem that enables PFQIM to analyze the dynamics of quadratic polynomials. It is observed that if the value of q is very close to one, then the method becomes more stable and converges faster. However, one limitation is that the method does not work for $q = 1$. Numerical experiments further demonstrated that PFQIM performs better than the corresponding classical iterative methods. The role of strange fixed points is clearly visualized in the dynamical planes. Both parameters q and δ showed strong stability behavior for various values. Moreover, since real dynamics differ from complex dynamics, they should be studied separately. The convergence plane proved to be a useful tool for visualizing the real dynamics of q-iterative methods.

Funding

This research received no external funding.

Conflicts of Interest

All authors jointly worked on the results, and they read and approved the final manuscript. Also, they declare that they have no competing interests.

References

[1] Alawaideh, Y. M., Lupas, A. A., Al-Khamiseh, B. M., Yousif, M. A., Mohammed, P. O. and Hamed, Y. S., *Hamiltonian formulation for continuous systems with second-order derivatives: a study of Podolsky generalized electrodynamics*, Axioms, 13(10) (2024), 665.

[2] Babajee, D. K. R., Cordero, A. and Torregrosa, J. R., *Study of iterative methods through the Cayley quadratic test*, J. Comput. Appl. Math., 291 (2016), 358–369.

[3] Bronshtein, I. N., Musiol, G., Semendyayev, K. A. and Mühlig, H., *Handbook of mathematics*, Springer, Berlin, 2015.

[4] Campos, B., Cordero, A., Torregrosa, J. R. and Vindel, P., *Dynamics of the family of c-iterative methods*, Int. J. Comput. Math., 92 (2014), 1–11.

[5] Chicharro, F. I., Cordero, A. and Torregrosa, J. R., *Drawing dynamical and parameters planes of iterative families and methods*, Sci. World J., (2013), 23566140.

[6] Cordero, A. and Torregrosa, J. R., *Variants of Newton's method using fifth-order quadrature formulas*, Appl. Math. Comput., 190(1) (2007), 686–698.

[7] Cordero, A., Torregrosa, J. R. and Vindel, P., *Dynamics of a family of Chebyshev–Halley type methods*, Appl. Math. Comput., 219(16) (2013), 8568–8583.

[8] Hernández, M. A. and Salanova, M. A., *A family of Chebyshev–Halley type methods*, Int. J. Comput. Math., 47(1–2) (1993), 59–63.

[9] Jackson, F. H., *A q-form of Taylor's formula*, Messenger Math., 38 (1909), 62–64.

[10] Jing, S. C. and Fan, H. Y., *q-Taylor's formula with its q-remainder*, Commun. Theor. Phys., 23(1) (1995), 117.

[11] Lee, M. and Kim, Y. I., *The dynamical analysis of a uniparametric family of three-point optimal eighth-order multiple-root finders under the Möbius conjugacy map on the Riemann sphere*, Numer. Algorithms, 83(3) (2020), 1063–1090.

[12] Magreñán, Á. A., *A new tool to study real dynamics: the convergence plane*, Appl. Math. Comput., 248 (2014), 215–224.

[13] Magreñán, Á. A., Cordero, A., Gutiérrez, J. M. and Torregrosa, J. R., *Real qualitative behavior of a fourth-order family of iterative methods by using the convergence plane*, Math. Comput. Simul., 105 (2014), 49–61.

[14] Magreñán, Á. A. and Gutiérrez, J. M., *Real dynamics for damped Newton's method applied to cubic polynomials*, J. Comput. Appl. Math., 275 (2015), 527–538.

[15] Maroju, P., Magreñán, Á. A., Sarría, Í. and Kumar, A., *Local convergence of fourth- and fifth-order parametric family of iterative methods in Banach spaces*, J. Math. Chem., 58(3) (2020), 1572–1589.

[16] Muhammad, B., Alawaideh, Y. M., Rehman, S. U., Yousif, M. A., Younas, U., Baleanu, D. and Mohammed, P. O., *Gross–Pitaevskii systems of fractional order with respect to multicomponent solitary wave dynamics*, Sci. Rep., 15(1) (2025), 24337.

[17] Nievergelt, Y., *Computing the distance from a point to a helix and solving Kepler's equation*, Nucl. Instrum. Methods Phys. Res. A, 598(3) (2009), 788–794.

[18] Nonlaopon, K., Khan, A. G., Ameen, F., Awan, M. U. and Cesarano, C., *Multi-step quantum numerical techniques for finding the solutions of nonlinear equations*, Mathematics, 10(15) (2022), 2227.

[19] Pavkov, T. M., Kabadzhov, V. G., Ivanov, I. K. and Ivanov, S. I., *Local convergence analysis of a one-parameter family of simultaneous methods with applications to real-world problems*, Algorithms, 16(2) (2023), 103.

[20] Román, C. E. C., *A new approach to study the dynamics of the modified Newton's method to multiple roots*, Bull. Math. Soc. Sci. Math. Roumanie, 62 (2019), 110.

[21] Sana, G., Mohammed, P. O., Shin, D. Y., Noor, M. A. and Oudat, M. S., *On iterative methods for solving nonlinear equations in quantum calculus*, Fractal Fract., 5(60) (2021).

[22] Sana, G., Noor, M. A. and Baleanu, D., *Novel higher-order iterative schemes based on the q-calculus for solving nonlinear equations*, AIMS Math., 7(3) (2021), 2473–2498.

[23] Singh, P., Mishra, P. K. and Pathak, R. S., *q-iterative methods*, IOSR J. Math., 9(1) (2013), 06–13.